

CHEMICAL STRUCTURE, SUBSTITUTION EFFECT, AND DRUG-LIKENESS APPLIED TO QUERCETIN AND ITS DERIVATIVES

Abderrahmane Rouane^{1,3}, Noureddine Tchouar², Salah Belaidi^{3*}, Aicha Kerassa^{4,3}, Touhami Lanez⁴

¹Department of Chemistry Physics, Laboratory of Modeling and Optimization of Industrial Systems, Faculty of Chemistry, University of USTO-MB, Algeria

²Laboratoire Génie des Procédés et Environnement (GPE), Faculté de chimie, Université des sciences et technologies d'Oran (USTO), Algérie

³Group of Computational and Pharmaceutical Chemistry, Laboratory of Molecular Chemistry and environment, Department of Chemistry, University of Biskra, Algeria

⁴VTRS Laboratory, Faculty of Sciences and Technology, University of El Oued, Algeria

Received: 20 October 2022 / Accepted: 22 November 2022 / Published online: 25 November 2022

ABSTRACT

In the current study, molecular geometry, electronic structure, effect of the substitution, and structure physical-chemistry relationship for Quercetin derivatives have been studied by DFT (B3LYP) theory and Hartree-Fock (HF). The calculated values, net charges, MESP contours/surfaces have also been drawn to explain the electronic reactivity of Quercetin, bond lengths, dipole moments, heats of formation, QSAR properties, Lipinski's parameters, Ligand efficiency (LE), Lipophilic Efficiency (LipE), are reported and discussed, to understand the biological activity of the Quercetin Derivatives.

Keywords: Quercetin, Anti-Malaria activity, SAR, drug-like, Lipinski rule, HF, DFT,

Author Correspondence, e-mail: prof.belaidi@mail.com

doi: <http://dx.doi.org/10.4314/jfas.1278>

1. INTRODUCTION

Flavonoids are many natural compounds; recently these compounds are considered an interesting scientific topic and fructified through the various biological and medical roles [1].

The one compounds Quercetin flavonoid that has antioxidant biological activity and cancer [2,3], it has a definite geometric structure [4.5], the effect of antioxidant Quercetin is attributed to the formation of stable, aryloxyl radical, it is due to the double bond ($C_2 = C_3$) that follows the geometric planarity, cyclic chains A and B in flavonoids is stabilized by the conjugate form [6-9].

The process of drug development is time-consuming and cost-intensive. Several years are required for lead identification, optimization, *in vitro* and *in vivo* testing before starting the first clinical trials [10-14]. Drug discovery activities are producing ever-larger volumes of complex data that carry significant levels of uncertainty; multi-parameter optimization methods enable this data to be better utilized to quickly target compounds with a good balance of properties, but they all have their strengths and weaknesses [15]. Therefore, we can use the multi-parameter optimization (MPO) methods to predict the best balance of properties, among these methods we carry out rules of thumb and calculated metrics.

Rules of thumb are the most common approach used to consider the quality of compounds relative to criteria beyond potency that provides guidelines regarding desirable compound characteristics. Several rules have been proposed; the most commonly used are Lipinski and Veber rules [16-17]. On the other hand, calculated metrics aim to combine the potency with other parameters into a single metric which may be monitored during optimization. The earliest and most commonly applied metrics are the Ligand Efficiency (LE) and the Lipophilic Efficiency (LipE) [17].

In this work, we have investigated the geometry, electronic structure and substituent effect [18] for Quercetin. Finally, we have studied some of QSAR proprieties [19-24] and drug likeness [25-28] proprieties of a series of Quercetin derivatives reported in literature.

2. MATERIALS AND METHODS

The molecular modeling calculation for all the Quercetin derivatives are performed by

HyperChem version 8.0.6 [29] and Gaussian 09 [30], MarvinSketch 15.8.3 [31] and Molinspiration online database [32].

Initially, the investigated molecules were pre-optimized by means of the Molecular Mechanics Force Field (MM+), ($\text{rms} = 0.01 \text{ Kcal}/\text{\AA}$). After that, the resulted minimized structures were further refined using the semi-empirical PM3 method.

In the next step, we realized the calculation of some geometric and electronic parameters, using various computational levels, HF and DFT/B3LYP with 6-311+G(d,p) and cc-pVDZ basis. This work also includes calculation of 3D MESP surface map and 2D MESP contour map to reveal the information regarding charge transfer within the molecule [33].

The calculation of QSAR properties is performed by the module QSAR Properties, QSAR Properties is a module, that together with HyperChem (version8.0.6), allows several properties commonly used in QSAR studies to be calculated.

Molinspiration, web-based software was used to obtain parameter such as TPSA (topological polar surface area), nrotb (number of rotatable bonds), HBA, HBD and drug likeness.

3. RESULTS AND DISCUSSION

3.1. Electronic Structure of Quercetin:

The optimized geometrical parameters of Quercetin [Fig. 1] are obtained using *ab-initio*/HF and DFT methods, listed in [Table I]and [Table II] with the experimental results [34] which are approximately similar to the theoretical results, regarding bond length and dihedral angles. From that, we can say the DFT/B3LYP method with(cc-pVDZ) base is more appropriate for further study on Quercetin and its derivatives.

Table I. Bond lengths of Quercetin

Parameters	HF/6-311G+d,p	DFT/6-311G+d,p	DFT/cc-pVDZ	HF/cc-pVDZ	Exp [34]
C1-C2	1.384	1.393	1.401	1.388	1.386
C1-C6	1.380	1.388	1.401	1.388	1.389
C2-C3	1.394	1.402	1.393	1.383	1.400
C2-O19	1.336	1.360	1.407	1.397	1.358
C3-C4	1.377	1.387	1.358	1.337	1.360
C4-C5	1.413	1.422	1.393	1.377	1.419

C4-O18	1.322	1.341	1.425	1.413	1.364
C5-C6	1.393	1.405	1.339	1.323	1.391
C5-C10	1.441	1.433	1.409	1.397	1.421
C6-O7	1.336	1.358	1.434	1.440	1.369
O7-C8	1.357	1.373	1.361	1.337	1.368
C8-C9	1.338	1.368	1.374	1.342	1.360
C8-C11	1.476	1.465	1.464	1.479	1.474
C9-C10	1.459	1.449	1.452	1.462	1.440
C9-O20	1.345	1.356	1.356	1.345	1.355
C10-O17	1.217	1.257	1.262	1.221	1.268
C11-C12	1.389	1.406	1.410	1.393	1.393
C11-C16	1.398	1.408	1.415	1.401	1.397
C13-C14	1.378	1.388	1.394	1.380	1.373
C14-C15	1.392	1.402	1.410	1.392	1.386
C14-O29	1.342	1.373	1.357	1.342	1.385
C15-C16	1.373	1.384	1.386	1.373	1.390
C15-O24	1.360	1.363	1.376	1.360	1.384
O18-H26	0.941	0.963	0.996	0.941	0.914
O19-H27	0.952	0.987	0.969	0.952	0.948
O20-H28	0.947	0.977	0.984	0.947	0.906
O24-H31	0.940	0.966	0.968	0.940	0.990
O29-H32	0.943	0.963	0.972	0.943	0.975

Table 2. Dihedral angles of Quercetin

Parameters	HF/6-311G+(d, p)	DFT/6-311G+(d, p)	DFT/cc- pVDZ	HF/ccpVDZ
C6-C1-C2-C3	000.0	000.0	-000.0	-000.0
C6-C1-C2-O19	179.9	180.0	180.0	179.9
H21-C1-C2-C3	-179.7	180.0	180.0	-179.7
H21-C1-C2-O19	000.2	-000.0	000.0	000.2
C2-C1-C6-C5	-000.0	000.0	000.0	-000.0
C2-C1-C6-C7	-179.9	180.0	180.0	-179.9
H21-C1-C6-C5	179.6	-180.0	180.0	179.7
H21-C1-C6-C7	-000.2	000.0	000.0	-000.2
C1-C2-C3-C4	000.0	000.0	-000.0	000.0
C1-C2-C3-H22	-179.9	180.0	180.0	-179.9
O19-C2-C3-C4	-179.9	180.0	-180.0	-179.9
O19-C2-C3-H22	000.0	-000.0	000.0	000.0
C1-C2-O19-H27	-179.6	179.9	-179.9	-179.8
C3-C2-O19-H27	000.3	-000.0	000.0	000.1
C2-C3-C4-C5	-000.0	000.0	000.0	000.0
C2-C3-C4-O18	-179.9	180.0	-180.0	-179.9
H22-C3-C4-C5	179.9	-180.0	180.0	-179.9

H22-C3-C4-O18	000.0	000.0	-000.0	000.0
C3-C4-C5-C6	-000.0	000.0	-000.0	-000.0
C3-C4-C5-C10	-179.9	180.0	-180.0	-179.9
O18-C4-C5-C6	179.8	-180.0	180.0	179.9
O18-C4-C5-C10	-000.0	-000.0	000.0	000.0
C3-C4-O18-H26	179.7	-180.0	179.9	179.8
C5-C4-O18-H26	-000.1	000.0	-000.0	-000.1
C4-C5-C6-C1	000.1	-000.0	000.0	000.0
C4-C5-C6-O7	-179.9	-180.0	-180.0	179.9
C10-C5-C6-C1	-179.9	-180.0	179.9	179.9
C10-C5-C6-O7	-00.0	000.0	-000.0	-000.1
C4-C5-C10-C9	179.8	-180.0	179.9	179.8
C4-C5-C10-O17	000.4	-000.0	000.0	000.2
C6-C5-C10-C9	-000.0	000.0	000.0	000.0
C6-C5-C10-O17	-179.5	179.9	-179.9	-179.6
C1-C6-O7-C8	179.8	180.0	-179.9	179.9
C5-C6-O7-C8	-000.0	000.0	000.0	000.0
C6-O7-C8C9	000.2	000.0	-000.0	000.2
C6-O7-C8-C11	179.4	-179.9	179.9	179.5
O7-C8-C9-C10	-000.3	000.0	000.0	-000.3
O7-C8-C9-O20	179.2	-179.9	-180.0	179.4
C11-C8-C9-C10	-179.3	179.9	180.0	-179.5
C11-C8-C9-O20	000.3	000.0	000.0	000.2
O7-C8-C11-C12	163.2	-179.8	180.0	166.2
O7-C8-C11-C16	-016.3	000.1	000.0	-013.4
C9-C8-C11-C12	-017.7	000.1	000.0	-014.4
C9-C8-C11-C15	162.6	-179.8	180.0	165.8
C8-C9-C10-C5	000.2	000.0	000.0	000.2
C8-C9-C10-O17	179.7	-179.9	180.0	179.8
O20-C9-C10-C5	-179.4	179.9	-179.9	-179.5
O20-C9-C10-O17	000.0	000.0	000.0	000.0
C8-C9-O20-H28	-178.3	180.0	-179.9	-178.8
C10-C9-O20-H28	001.3	000.0	000.0	000.9
C8-C11-C12-C13	-179.6	180.0	180.0	-179.7
C8-C11-C12-H23	000.2	000.0	000.0	000.0
C16-C11-C12-C13	-000.0	000.0	000.0	-000.0
C16-C11-C12-H23	179.8	-180.0	180.0	179.74
C8-C11-C16-C15	-179.9	-180.0	-180.0	-179.9
C8-C11-C15-H25	-000.0	000.0	000.0	-000.0
C12-C11-C15-C16	000.4	-000.0	-000.0	000.3
C12-C11-C16-H25	-179.6	179.9	-180.0	-179.7
C11-C12-C13-C14	-000.2	000.0	000.0	-000.2
C11-C12-C13-H30	179.6	180.0	-180.0	179.7
H23-C12-C13-C14	179.8	180.0	180.0	179.9

H23-C12-C13-H30	-000.2	000.0	000.0	-000.0
C12-C13-C14-C15	000.2	000.0	000.0	000.2
C12-C13-C14-O29	-179.8	179.9	-180.0	-179.8
H30-C13-C14-C15	-179.7	-180.0	-180.0	-179.7
H30-C13-C14-O29	000.1	000.1	000.0	000.1
C13-C14-C15-C16	000.1	180.0	000.0	000.0
C13-C14-C15-O24	180.0	-179.9	180.0	179.9
O29-C14-C16-C15	-179.7	180.0	180.0	-179.8
O29-C14-C16-O25	000.1	000.0	000.0	000.0
C13-C14-O29-H32	180.0	000.1	-179.9	179.9
C15-C14-O29-H32	-000.1	-179.8	000.0	-000.1
C11-C16-C15-C14	-000.4	000.0	000.0	-000.3
C11-C16-C15-O24	179.6	-180.0	-180.0	179.7
H25-C16-C15-C14	179.6	179.9	-180.0	179.7
H25-C16-C15-O24	-000.2	000.0	000.0	-000.1
C14-C15-O24-H31	179.8	000.0	-179.9	179.8
C16-C15-O24-H31	-000.3	-179.9	000.0	-000.2

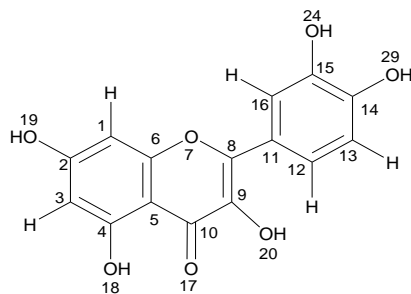


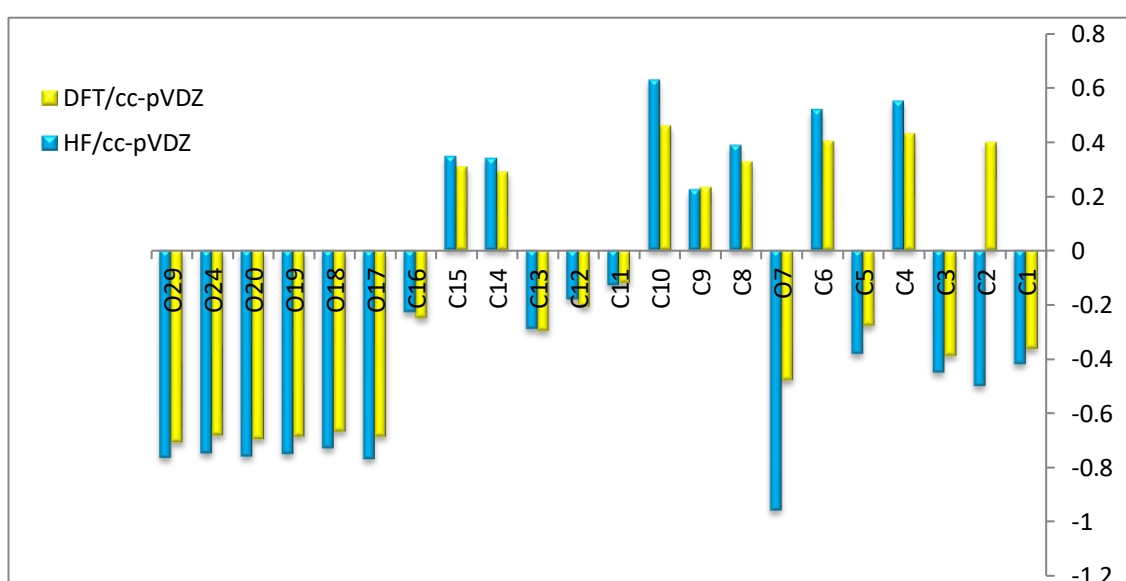
Fig.1. Structure of Quercetin

The atomic charge calculation depicting the charges of every atom in the molecule is vital as these influence bond lengths between the atoms. Atomic charges affect dipole moment, molecular polarizability, electronic structure, acidity–basicity behavior of molecular systems and electrostatic potential surfaces [35-38].

The atomic charges obtained from NBO population analysis are listed in [Table III]. According to NBO, the two methods predict the same tendencies except for C2 atom as shown in Fig.2.

Table 3. NBO charges of Quercetin

Atoms	DFT/cc-pVDZ	HF/cc-pVDZ
C1	-0.363	-0.420
C2	0.399	-0.500
C3	-0.390	-0.450
C4	0.432	0.552
C5	-0.279	-0.382
C6	0.405	0.521
O7	-0.479	-0.96
C8	0.329	0.389
C9	0.234	0.224
C10	0.461	0.630
C11	-0.119	-0.129
C12	-0.208	-0.182
C13	-0.296	-0.290
C14	0.291	0.341
C15	0.310	0.348
C16	-0.249	-0.228
O17	-0.688	-0.770
O18	-0.668	-0.730
O19	-0.687	-0.751
O20	-0.697	-0.761
O24	-0.683	-0.748
O29	-0.708	-0.766

**Fig.2.**NBO population analysis of Quercetin

3.2. Molecular electrostatic potential

The molecular electrostatic potential surface (MESP) which is a plot of electrostatic potential mapped onto the isoelectron density surface simultaneously displays molecular shape, size and electrostatic potential values and has been plotted for both the molecules. Molecular electrostatic potential (MESP) mapping is very useful in the investigation of the molecular structure with its physiochemical property relationships [39-44].

In this study, the electrostatic potentials at the surface are presented by different colors [Fig.3]. Red color parts represent the regions of negative electrostatic potential while blue ones represent regions of positive electrostatic potential. Green color parts represent also regions of zero potential.

A portion of the molecule that has a negative electrostatic potential is susceptible to electrophilic attack while the positive ones are related to nucleophilic reactivity.

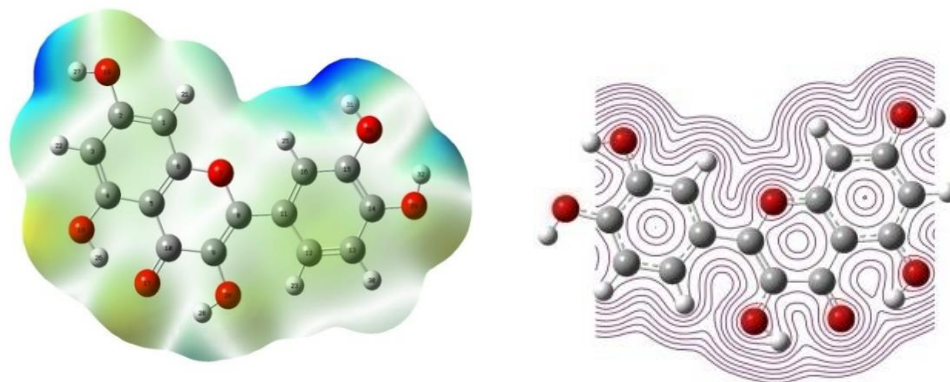


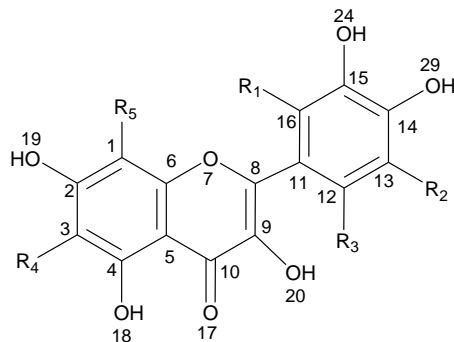
Fig.3. 2D MESP and 3D MESP contour map for Quercetin

3.3. Substitution Effect on Quercetin Structure

For the effect of the substitution, we have studied two series [Fig.4], the methyl group for the first series (an electron donor group) and the methoxy group for the second one (an electron attractor group).

The obtained results of heat of formation, dipole moment (μ), HOMO (the Highest Occupied Molecular Orbital) and LUMO (The Lowest Unoccupied Molecular Orbital) energies are listed in [Table IV]. In [Table V], [Table VI] Net atomic charges are also reported.

The heat of formation for Quercetin derivatives, compared to the general structure of Quercetin,



Series 1

- GS R1=R2=R3=R4=R5=H
 A1 R1=CH₃, R2=R3=R4=R5
 A2 R1=H, R2=CH₃, R3=R4=R5=H
 A3 R1=R2=H, R3=CH₃, R4=R5=H
 A4 R1=R2= R3=H, R4=CH₃, R5=H
 A5 R1=R2=R3=R4=H, R5=CH₃

Series 2

- GS R1=R2=R3=R4=R5=H
 B1 R1=OCH₃, R2=R3=R4=R5
 B2 R1=H, R2=OCH₃, R3=R4=R5=H
 B3 R1=R2=H, R3=OCH₃, R4=R5=H
 B4 R1=R2= R3=H, R4=OCH₃, R5=H
 B5 R1=R2=R3=R4=H, R5=OCH₃

Fig.4. Quercetin systems

Table 4. Energies of Quercetin derivatives

Compound	Heat of Formation kcal/mol	HOMO (a.u.)	LUMO (a.u.)	ΔE (a.u.)	μ (D)
GS	-214.27	-0.246	-0.007	0.23	2.663
A1	-219.11	-0.244	0.005	0.23	2.814
A2	-221.49	-0.104	-0.124	0.01	2.854
A3	-219.39	-0.242	-0.006	0.23	2.947
A4	-220.35	-0.245	-0.006	0.23	2.174
A5	-220.53	-0.246	-0.005	0.24	2.876
B1	-247.05	-0.253	-0.003	0.24	3.831
B2	-252.54	-0.246	-0.007	0.23	2.165
B3	-247.57	-0.251	-0.0008	0.25	4.231
B4	-250.24	-0.246	-0.008	0.23	2.641
B5	-246.72	-0.245	-0.006	0.23	2.774

Note: Heat of formation calculated by PM3 (HyperChem 8.0.6), HOMO, LUMO, ΔE, μ calculated by DFT/B3LYP (Gaussien 09).

decreased about 5.90 (Kcal/mol) at each addition of methoxy and about 34.55 (Kcal/mol) at each addition of methyl.

On the other hand, in smaller HOMO–LUMO gap, there is easy flow of electrons to the higher energy state making it softer and more reactive (HSAB principle: hard and soft acids and bases). Hard bases have highest-occupied molecular orbitals (HOMO) of low energy, and hard acids have lowest-unoccupied molecular orbitals (LUMO) of high energy [45].

Among the various substituted that we have added each time to Quercetin and by the calculations that we have performed, it was found that electron donors of compound A2 has the lowest energy gap HOMO-LUMO (0.019a.u) for the first series and shows the value of the dipole moment.(2.854 D) and compound B4 has the lowest energy gap (0.23 a.u)for the second series and shows the value of the dipole moment(2.641 D) in the [Table IV].So, The carbon C3 relative to compound A2 shows the maximum negative NBO charge (-0.399). This site is relative to the preferential electrophilic attack. For compounds B4, the maximum positive NBO charges is in carbon C3 (0.181). This is site relative to the preferential nucleophilic attack.

We also note that the methyl substituent (donor effect) has the effect of increasing the energy of the HOMO, with little change in the LUMO, which make the compound A2 soft base, for the chloride and cyanide substituents (acceptor effect) has the effect of decreases the energy of the LUMO, which make the compound B3 soft acid.

The negative atomic charge on C3 and O7 take the values (-0.399) and (-0.496) respectively in the compound A2, these positionsC3and O7 with the important negative charges lead to preferential site of electrophilic attack for the first series [Table V], also for compound B3 for the second series, The positive atomic charge on C10 (0.464) as shown in [Table VI], this position C10 with the important positive charge led to preferential site of nucleophilic attack.

The contour plots of the π -like frontier orbital's for the ground state of compound A2 are shown in [Fig.5], including the highest occupied molecular orbital (HOMO) and lowest unoccupied molecular orbital (LUMO). From the plots, one can find that the HOMO mainly concentrates on C11 and the Cromone ring with some delocalization along C8, C12 and C16, whereas, the LUMO mainly concentrates on C14 with some delocalization along O29, C13 and C15. These further demonstrate that there exists the delocalization of the conjugated π -electron system in the molecule of compound A2.

Table 5. NBO charges of Quercetin series 1

Atoms	GS	A1	A2	A3	A4	A5
C1	-0.363	-0.364	-0.363	-0.363	-0.356	-0.159
C2	0.399	0.398	0.399	0.399	0.406	0.401
C3	-0.390	-0.390	-0.399	-0.390	-0.182	-0.383
C4	0.432	0.431	0.431	0.432	0.429	0.425
C5	-0.279	-0.28	-0.279	-0.281	-0.272	-0.272
C6	0.405	0.408	0.405	0.403	0.401	0.410
O7	-0.479	-0.481	-0.496	-0.490	-0.497	-0.501
C8	0.329	0.235	0.331	0.326	0.329	0.329
C9	0.234	0.231	0.233	0.229	0.234	0.235
C10	0.461	0.464	0.461	0.466	0.461	0.462
C11	-0.119	-0.116	-0.113	-0.116	-0.119	-0.118
C12	-0.208	-0.194	-0.210	-0.006	-0.208	-0.208
C13	-0.296	-0.303	-0.097	-0.296	-0.297	-0.296
C14	0.291	0.297	0.295	0.298	0.290	0.290
C15	0.310	0.309	0.316	0.303	0.310	0.310
C16	-0.249	-0.042	-0.253	-0.236	-0.249	-0.250
C-R1	-	-0.657	-	-	-	-
C-R2	-	-	-0.671	-	-	-
C-R3	-	-	-	-0.656	-	-
C-R4	-	-	-	-	-0.682	-
C-R5	-	-	-	-	-	-0.657

Note: NBO charges calculated by DFT (Gaussien 09).

Table 6. NBO charges of Quercetin Series 2

Atoms	GS	B1	B2	B3	B4	B5
C1	-0.363	-0.364	-0.363	-0.364	-0.357	0.202
C2	0.399	0.398	0.399	0.397	0.369	0.356
C3	-0.390	-0.391	-0.390	0.391	0.181	-0.381
C4	0.432	0.431	0.431	0.431	0.371	0.420
C5	-0.279	-0.279	-0.279	-0.28	-0.268	-0.271
C6	0.405	0.404	0.405	0.403	0.396	0.367
O7	-0.479	-0.484	-0.495	-0.492	-0.495	-0.489
C8	0.329	0.33	0.330	0.324	0.331	0.332
C9	0.234	0.232	0.230	0.24	0.233	0.232
C10	0.461	0.463	0.461	0.464	0.495	0.461
C11	-0.119	-0.153	-0.105	-0.155	-0.119	-0.120
C12	-0.208	-0.192	-0.305	0.367	-0.208	-0.208

C13	-0.296	-0.31	0.282	-0.397	-0.296	-0.297
C14	0.291	0.296	0.255	0.307	0.291	0.291
C15	0.310	0.263	0.316	0.285	0.310	0.310
C16	-0.249	0.319	-0.266	-0.228	-0.249	-0.249
O-R1	-	-0.25	-	-	-	-
O-R2	-	-	-0.253	-	-	-
O-R3	-	-	-	-0.258	-	-
O-R4	-	-	-	-	-0.248	-
O-R5	-	-	-	-	-	-0.246

Note: NBO charges calculated by DFT (Gaussien 09).

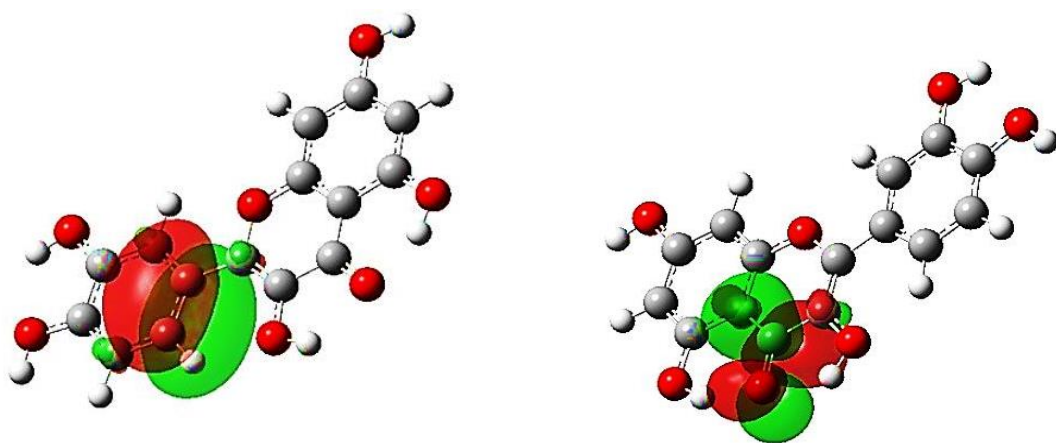
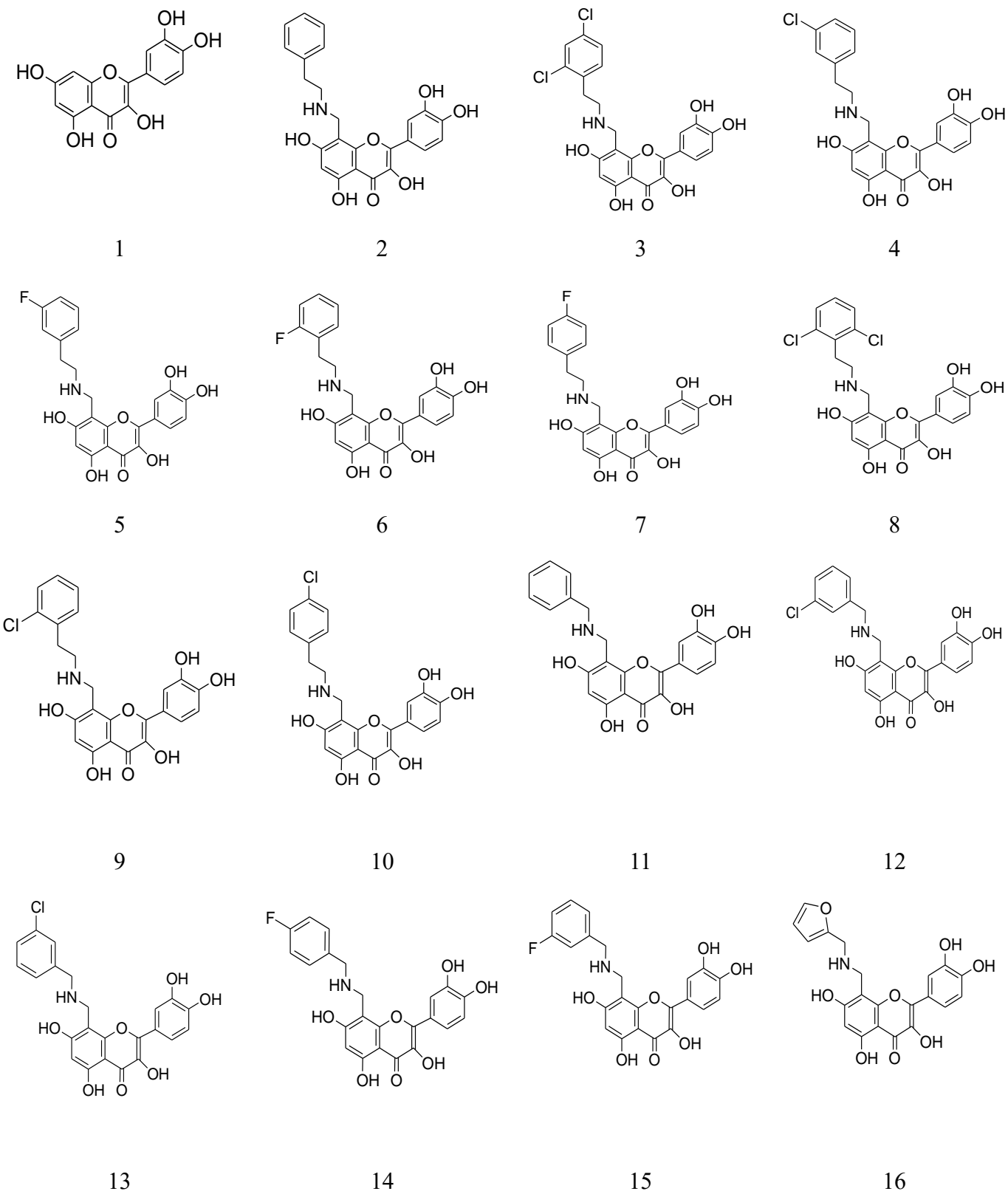


Fig.5. HOMO and LUMO for compound A2

3.4. Structure Activity/Property Relationship for Quercetin Derivatives

Based on our conclusions on the effect of substitution on the Quercetin. We chose a series of Quercetin derivatives, having anti-malaria activity [46-51].

For the series of Quercetin derivatives [Fig.6] we have studied seven physicochemical properties. The properties involved are: Surface area grid (SAG), molar volume (V), hydration energy (HE), partition coefficient octanol/water (logP), molar refractivity (MR), polarizability (Pol) and molecular weight (MW). The results using HyperChem 8.0.6 software are shown in [Tables VII], and others were calculated using Molinspiration online database (TPSA and nrotb). For example, [Fig.VII] shows the favored conformation in 3D of the compound 4. We will continue this work in the future by a quantitative calculation.



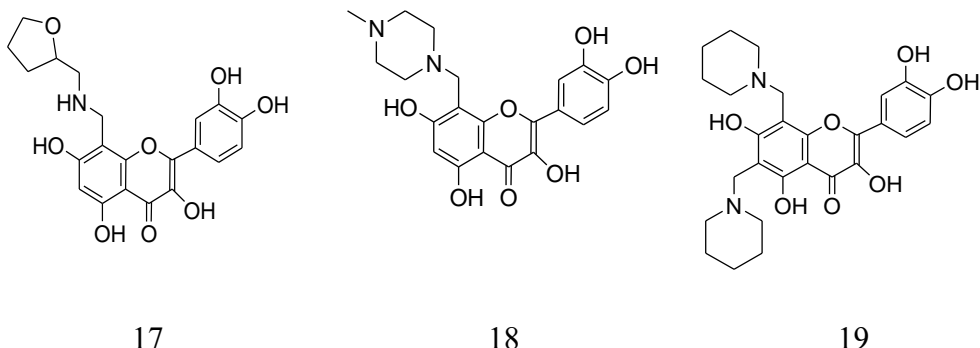


Fig.6. 2D structures of Quercetin derivatives

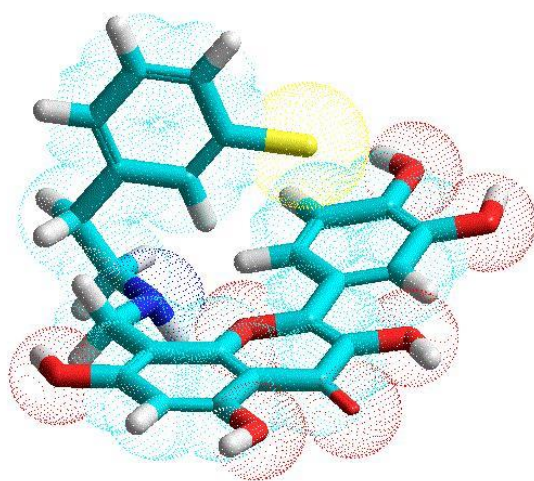


Fig.7. 3D Conformation of compound 4 (HyperChem 8.0.6)

Molecular Polarizability of a molecule characterizes the capability of its electronic system to modulate itself on the application of external field, and it plays an important role in modeling many molecular properties and biological activities. [52] The polarizability of the molecule depends only on its volume. Molecular volume determines transport characteristics of molecules, such as intestinal absorption or blood-brain barrier penetration. Volume is therefore often used in QSAR studies to model molecular properties and biological activity.

The molar refractivity is a steric parameter that is dependent on the spatial array of the aromatic ring in the synthesized compounds. The spatial arrangement also is necessary to study the interaction of the ligand with the receptor. [53] Molar refractivity is related, not only to the volume of the molecules but also to the London dispersive forces that act in the drug receptor

interaction.

Hydration energy is a key factor determining the stability of different molecular conformations in water solutions [54].

In the biological environments the polar molecules are surrounded by water molecules. They are establishing hydrogen bonds between a water molecule and these molecules. The donor sites of proton interact with the oxygen atom of water, and the acceptor sites of proton interact with the hydrogen atom.

We observe that polarizability data are generally proportional to refractivity, molecular volume and surface. Compound number 19 shows the maximum value of both (polarizability (51.72 \AA^3) and refractivity (143.02 \AA^3). This compound has also high values of Molecular weight (496.56 uma), volume (1300.46 \AA^3) and surface (713.88 \AA^2). Compound 16 indicates the maximum absolute value of hydration energy (32.970Kcal/mol). Regarding to compound 19, it shows the minimum absolute value (19.650 Kcal/mol). In fact, hydrophobic molecule of Quercetin derivatives leads to the decrease of the hydration energy. Contrariwise, the presence of hydrophilic groups in the compound number 16, having 8 (HBD): and 5 (HBA): (5OH, three cyclic 2O) leads to the increase of the hydration energy, and for compound 19 having 10(HBD) and 5 (HBA).

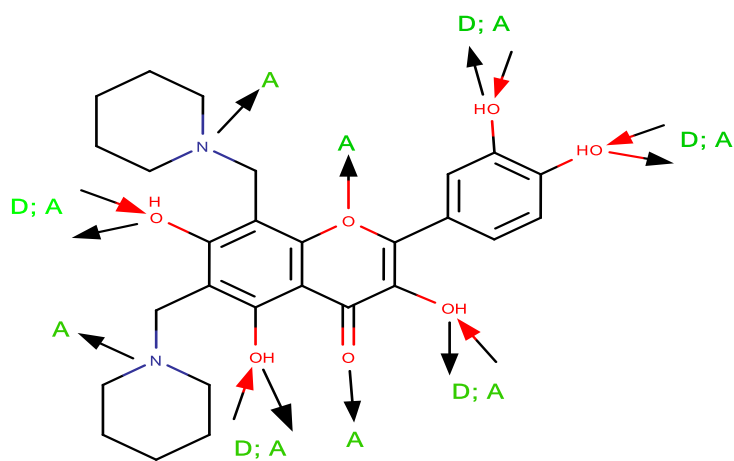


Fig.8. donors (D) and acceptors (A) of compound 19

Number of rotatable bonds (nrotb) is a simple topological parameter that measures molecular flexibility and is considered to be a good descriptor of oral bioavailability of drugs.¹⁷ The number of rotatable bonds (nrotb) was defined as any single bond, not in a ring, bound to a non-terminal heavy (i.e., non-hydrogen) atom. Excluded from the count were amide C–N bonds because of their high rotational energy barrier. The low number of rotatable bonds (reduced flexibility) in the studied series indicates that these Ligands upon binding to a protein change their conformation only slightly. Rotatable bonds are under 10 so all the screened compounds were flexible.

Topological polar surface area (TPSA) is a very useful parameter for prediction of drug transport properties. Polar surface area is defined as a sum of surfaces of polar atoms (usually oxygens, nitrogens and attached hydrogens) in a molecule. This parameter has been shown to correlate very well with the human intestinal absorption, Caco-2 monolayer's permeability, and blood-brain barrier penetration. [55]

Molecules with PSA values of 140 \AA^2 or more are expected to exhibit poor intestinal absorption. [56]

TPSA of Quercetin derivatives were found in the range of 131.35- 156.52. In our case, all compounds chosen have TPSA above 140 \AA^2 , except compounds 1, 18 and 19 have TPSA under 140 \AA^2 , [Table VII].

All the screened compounds were flexible, especially, compounds 2,3 and 5-10 which have 6 rotatable bonds [Table VII].

Table 7. QSAR proprieties for Quercetin Derivatives

Compound	Molecular weight (amu)	molecular surface (\AA^2) grid	molecular volume (\AA^3)	Polarizability (\AA^3)	Refractivity (\AA^3)	Hydration Energy (Kcal/mol)	nrotb	TPSA (\AA^2)
1	302.24	466.76	754.13	28.54	83.17	-32.51	0	131.35
2	435.43	643.55	1133.84	45.06	129.16	-29.52	6	143.38
3	504.32	662.19	1194.56	48.91	138.60	-29.50	6	143.38
4	469.88	668.53	1176.23	46.99	133.88	-28.91	1	143.38
5	453.42	652.12	1143.30	44.97	129.29	-28.95	6	143.38
6	453.42	629.76	1126.86	44.97	129.29	-29.84	6	143.38
7	453.42	654.28	1142.47	44.97	129.29	-28.88	6	143.38

8	504.32	647.57	1194.37	48.91	138.60	-28.37	6	143.38
9	469.88	643.52	1152.85	46.99	133.88	-29.82	6	143.38
10	469.88	668.65	1175.78	46.99	133.88	-28.85	6	143.38
11	421.41	642.40	1099.75	43.22	124.41	-30.58	5	143.38
12	455.85	667.24	1142.96	45.15	129.13	-30.21	5	143.38
13	455.85	662.75	1142.34	45.15	129.13	-30.20	5	143.38
14	439.40	644.88	1109.97	43.13	124.54	-29.93	5	143.38
15	439.40	647.99	1110.58	43.13	124.54	-30.26	5	143.38
16	411.37	617.11	1050.69	40.38	115.26	-32.97	5	156.52
17	415.40	629.68	1077.12	40.77	113.91	-29.48	5	152.61
18	414.41	598.58	1055.00	41.48	117.00	-25.68	3	137.83
19	496.56	713.88	1300.46	51.72	143.02	-19.65	3	137.83

3.5. Multi-Parameter Optimization (MPO) and drug-likeness of Quercetin Derivatives

An important objective for this communication was to evaluate the physicochemical domain on nineteen derivatives of Quercetin [Fig.6]. The properties involved are: Partition coefficient octanol/water ($\log P$), molecular weight (MW), hydrogen bond donors (HBD), hydrogen bond acceptors (HBA), number of rotatable bonds (nrobt), polar surface area (PSA), Ligand efficiency (LE) and Lipophilic efficiency (LipE). The results were calculated using HyperChem8.0.6, and Molinspiration online database are shown in [Table VIII].

In this part, we have studied Lipinski to identify “drug-like” compounds. This last appears as a promising paradigm to encode the balance among the molecular properties of a compound that influences its pharmacodynamics and pharmacokinetics and ultimately optimizes their absorption, distribution, metabolism and excretion (ADME) in human body like a drug. The empirical conditions to satisfy Lipinski’s rule and manifest a good oral bioavailability involve a balance between the aqueous solubility of a compound and its ability to diffuse passively through the different biological barriers [57,58].

These parameters allow ascertaining oral absorption or membrane permeability that occurs when the evaluated molecule follows Lipinski’s rule of five since molecular weight (MW) $\leq 500\text{Da}$, an octanol water partition coefficient $\log P \leq 5$, H-bond donors, nitrogen or oxygen atoms with one or more hydrogen atoms (HBD) ≤ 5 and H-bond acceptors, nitrogen or oxygen atoms (HBA) ≤ 10 . [59]

Table 8. Pharmacological activities and properties involved in MPO method for Quercetin derivatives

Compound	Lipinski rules					Ligand efficiency and Lipophilicity efficiency		
	molecular mass (amu)	LogP	HB	HBD	Rules of five violation	PIC5	LE	LipE
					A			
1	302.24	-4.01	7	5	0	5.535	0.352	9.545
2	435.43	-3.54	8	6	1	5.674	0.248	9.214
3	504.32	-3.98	10	6	2	7.146	0.294	11.126
4	469.88	-3.76	6	6	1	7.103	0.301	10.863
5	453.42	-4.14	9	6	1	6.888	0.292	11.028
6	453.42	-4.14	9	6	1	6.619	0.28	10.759
7	453.42	-4.14	9	6	1	6.533	0.277	10.673
8	504.32	-3.98	10	6	2	6.643	0.273	10.623
9	469.88	-3.76	9	6	1	6.534	0.277	10.294
10	469.88	-3.76	9	6	1	5.733	0.243	9.493
11	421.4	-3.79	8	5	1	5.662	0.255	9.452
12	455.85	-4.01	9	6	1	6.587	0.288	10.597
13	455.85	-4.01	9	6	1	6.227	0.272	10.237
14	439.39	-4.39	9	6	1	6.144	0.268	10.534
15	439.39	-4.39	9	6	1	6.159	0.269	10.549
16	411.37	-5.92	8	5	1	5.652	0.263	11.572
17	415.4	-4.57	9	5	1	5.656	0.263	10.226
18	414.41	-4.64	10	5	0	5.622	0.262	10.262
19	496.56	-3.42	10	5	0	5.923	0.285	9.343

Log P is used to predict the solubility of oral drug. If LogP increases, solubility in water decreases so absorption decreases. On one hand, a negative value for log P indicates that the compound is too hydrophilic. So, it has good aqueous-solubility, better gastric tolerance and efficient elimination through the kidneys. On the other hand, a positive value for log P indicates that the compound is too lipophilic. So it has a good permeability through biological membrane, a better binding to plasma proteins, elimination by metabolism but a poor solubility and gastric tolerance [59]. In our case, all the values of logP are negative, so they have a good solubility and a better gastric tolerance. Compound 19 has a maximum value of log p (-3.42).

The molecular weight is more than 500 DA for compounds 3 and 8. The smaller MW is, the

better the absorption will be. The other compounds have MW under 500 DA, thus, they can easily pass through cell membrane.

The compounds 1, 11, 16, 17, 18, 19 have 5 H-bond donors. If there is a small number of hydrogen bond donor, the fat solubility will be high and therefore the drug will be able to penetrate the cell membrane to reach the inside of the cell.

These are found to be within Lipinski's limit i.e., less than 10 and 5 respectively, in the tested compounds. Molecules violating more than one of these parameters may have problems with bioavailability and high probability of failure to display druglikeness [60].

The calculation results show that all compounds meet the Lipinski rules, suggesting that these compounds theoretically would not have problems with oral bioavailability, whereas, compounds 3 and 8 were found doesn't obey the Lipinski rule, suggesting that these compounds theoretically would have problems with oral bioavailability.

Ligand efficiency (LE) and Lipophilicity efficiency (LipE) are defined as follows:

$$\text{LE} = \frac{1}{4}\text{pIC50}/\text{NH} \quad (1)$$

Where: NH is the number of heavy atoms. So LE decreases with increasing number of heavy atoms.

$$\text{LipE} = \text{pIC50} - \log P \quad (2)$$

The lipophilicity is the major factor for the promiscuity of compounds, LipE optimized compounds should be more selective. It is suggested to target a LipE in a range of 5–7 or even higher. If LipE is between 5 and 9 or over 10, the optimized compounds are more selective.

We can see through the results in [TableVIII] that all compounds have LipE over 9, this indicates that all compounds were successfully optimized. Also, we can see that compound 1 had highest LE values of the data were deemed to be the most optimal compound.

4. CONCLUSION

The study of the structure of Quercetin based on ab initio and DFT prove that our calculated results are similar and very similar to experimental data taken from the literature. The comparison between donor group (methyl) and the acceptor group (methoxy) substitution of Quercetin showed an influence on the nature of the substitution on decreasing the heat of

formation of about 5.901 kcal/mol for the addition of methoxy and about 34.558 kcal/mol for the addition of methyl.

The compound A2 is predicted to be the most reactive compound with the least energy gap HOMO-LUMO of all flavonoids substituted compounds and respectively carbons C3 is the most preferential sites for nucleophilic attack.

The application of Lipinski rules leads us to conclude that most of our compounds, theoretically, will not have problems with oral bioavailability.

Compound 19 is expected to have the highest coefficient of partition ($\log P$); it has a good gastric tolerance. Compound 19 has important hydration energy; it has a better distribution in fabrics.

This section may be separated into 2 parts. The same data or information given in a Table must not be repeated in a Figure and vice versa. It is not acceptable to repeat extensively the numbers from Tables in the text or to give lengthy explanations of Tables or Figures. The final paragraph should highlight the main conclusions of the study.

6. REFERENCES

- [1] Silvia H., Taleb., Karin., Fernando B. C., Dionéia C. R. O., Detection of flavonoids in glandular trichomes of Chromolaena species (Eupatorieae, Asteraceae) by reversed-phase high-performance liquid chromatography., *Braz. J. Pharm.Sci*, 2007, 2, 43.
- [2] Pyrzynska K., Biesaga M., Trends. Analyt. Chem, 2009, 28, 894, doi: 10.1016/j.trac.2009.03.015
- [3] Dias T.A., Duarte C.L., Lima C.F., Proen  a M.F., Pereira W.C., *Eur. J. Med. Chem.*, 2013, 65, 500-510, doi: 10.1016/j.ejmech.2013.04. 064.
- [4] Belaidi S., Belaidi H., and Bouzidi D. , *Comput J. Theor. Nanosci.* 2015, 12, 1737-1745, doi : 10.1166/jctn.2015.3952
- [5] Belaidi S., Mazri R., Belaidi H., Lanez T., Bouzidi D., *Asian J. Chem.*, 2013, 25, 16, 9241, doi:10.14233/ajchem.2013.15199
- [6] Xiao J., Capanoglu E., Jassbi A., Miron A., *Biotechnol. Adv.*, 2014, 11, 2, doi:10.1016/j.biotechadv.2014.11.002
- [7] Boeck P., Falca  o C.A.B., Leal C.P., Yunes R.A., Filho V.C., Torres S.E.C., Rossi B.B.,

Bioorg. Med. Chem., 2006, 14, 1538–1545, doi: 10.1016/j.bmc.2005.10.005

[8] Beker B.Y., Bakır T., Sönmezoglu I., İmer F., Apak R., Chem. Phys. Lipids, 2011. 164, 732–739, doi: 10.1016/j.chemphyslip.2011.09.001

[9] Tarahovsky Y.S., Yagolnik E.A., Muzafarov E.N., Abdrasilov B.S., Kim Y.A., Biochim. Biophys. Acta., 2012, 1818, 695–702, doi: 10.1016/j.bbamem.2011.08.020.

[10] Yamauchi K., Mitsunaga T., Inagaki M., Suzuki T., Bioorg. Med. Chem., 2014, 22, 3331–3340, doi: 10.1016/j.bmc.2014.04.053

[11] Zakharov A., Lagunin A., Filimonov D., Poroikov V., J. Chem. Res. Toxicol., 2012. 25, 2378, doi: 10.1021/tx300247r

[12] Liao H., Changa Y., Linb Y., Yangb L., Chouc Y., Wangb B.B., QSAR Analysis of the Lipid Peroxidation Inhibitory Activity with Structure and Energetics of 36 Flavonoids Derivatives., J.Chin.Chem. Soc., 2006, 53, 1251-1261

[13] Ke T., Xiao Z.B., Xiao Q.L., Yue Z., Ji H.S., Chao W.T., DaHai H., J. Comput. In Theor. Nanosci., 2014, 11, 1785, doi:10.1166/jctn.2014.3567

[14] Is-ik E., S-ahin S., Demir C., Talanta, 2013, 111, 119–124, doi: 10.1016/j.talanta.2013.02.053

[15] Segall D.M., J. Curr. Pharma. Des., 2012, 18, 1292, doi: 10.2174/138161212799436430

[16] Lipinski C.A., Lombardo F., Dominy B.W., and Feeney P., Adv. Drug Deliv. Rev., 2012, 64, 4-17, doi: 10.1016/j.addr.2012.09.019

[17] Veber D.F., Johnson S.R., Cheng H.Y., Smith B.R., Ward K.W., and Kopple K.D., J. Med. Chem., 2002, 45, 2615, doi: 10.1021/jm020017n PMID: 12036371.

[18] Belaidi S, Almi Z., Bouzidi D., J. Comput. Theor. Nanosci., 2014, 11(12), 2481-2488, doi:10.1166/jctn.2014.3665

[19] Medjahed S., Belaidi S., Djekhaba S., Tchouar N., Kerassa A., J. Bionanosci., 2016, 10(2), 118-126, doi: 10.1166/jbns.2016.1358

[20] Belaidi S., Salah T., Melkemi N., Sinha L., Prasad O., J. Comput. Theor. Nanosci., 2015, 12(9), 2421-2427, doi: 10.1166/jctn.2015.4042

[21] Belaidi S., Lanez T., Omari M., Botrel A., Quantitative conformational analysis of dissymmetric macrolides by molecular modeling., Asian J. Chem., 2005, 17(2), 859-870

- [22] Melkemi N. and Belaidi S., J. Comput. Theor. Nanosci., 2014, 11, 801-806, doi:10.1166/jctn.2014.3431
- [23] Belaidi S., Youcef O., Salah T., and Lanez T., J. Comput. Theor. Nanosci. 2015, 12 (11), 4855-4861, doi:10.1166/jctn.2015.4451
- [24] Dermeche K., Tchouar N., Belaidi S., Salah T., J. Bionanosci. 2015, 9(5), 395-400, doi: 10.1166/jbns.2015.132025.
- [25] Rouane A., Tchouar N., Kerassa A., Cinar M., Belaidi S., J. Bionanosci. 2018, 12(2), 278-283, doi: 10.1166/jbns.2018.1511
- [26] Fouedjou R.T., Chtita S., Bakhouch M., Belaidi S., Ouassaf M., J. Biomol. Struct. Dyn., 2021, 1-15, doi: 10.1080/07391102.2021.1914170.
- [27] Ouassaf M., Belaidi S., Lotfy K., Daoud I., and Belaidi H., J. Bionanosci., 2018, 12,1-11, doi:10.1166/jbns.2018.1505
- [28] Belaidi H., Belaidi S., Katan C., Latouche C., Boucekkine A., J. Mol. Model., 2016, 22 (11), 1-8, doi: 10.1007/s00894-016-3132-8
- [29] HyperChem (Molecular Modeling System) Hypercube, Inc., 1115 NW, 4th Street, Gainesville, FL 32601, USA (2008).
- [30] Gaussian 09, Frisch M.J., Trucks G.W., Schlegel H.B., Scuseria G.E., Robb M.A., Cheeseman J.R., calmaniG.S, Barone V., Mennucci B., Petersson G.A., Nakatsuji, Caricato H.M., Li X.,Hratchian H.P., Izmaylov A.F., Bloino J., Zheng G., Sonnenberg J.L., Hada M., Ehara M., Toyota K., Fukuda R., Hasegawa J., Ishida M., Nakajima T., Honda Y., Kitao O., Nakai H., Vreven T., Montgomery J.A., Peralta J.E., Ogliaro F., Bearpark M., Heyd J.J., Brothers E.,Kudin K.N, Staroverov V.N., Keith T., Kobayashi R., Normand J., Raghavachari K., Rendell A., Burant J.C., Iyengar S.S., TomasiJ., Cossi M., Rega N., Millam J.M., Klene M., Knox J.E., Cross J.B., Bakken V., Adamo C., Jaramillo J., Gomperts R., Stratmann R.E., Yazyev O., Austin A., Cammi R., Pomelli C., Ochterski J.W., Martin R.L., Morokuma K., Zakrzewski V.G., Voth G.A., Salvador P., Dannenberg J.J., Dapprich S., Daniels A., Farkas O., Foresman J.B., Ortiz J.Z., Cioslowski J. and Fox D.J., Gaussian Inc., Wallingford, CT (2010).
- [31] MarvinSketch. Chemaxon (<http://www.chemaxon.com>),
- [32] Database, [<http://www.molinspiration.com>].

- [33] Kerassa A., Belaidi S., Harkati D., Lanez T., Prasad O., Sinha L., Rev. Theor. Sci., 2016, 4, 85-96, doi: 10.1166/rits.2016.1050
- [34] Xue Y., Gong X., J. Mol. Struc-Theochem., 2009, 901, 226, doi:10.1016/j.theochem.2009.01.034
- [35]. Sidir I., Sidir Y.G., Kumalar M., and Tasal E., J. Mol. Struct., 2010, 964, 134-151, doi: 10.1016/j.molstruc.2009.11.023
- [36] Balachandran V., and Parimala K., Spectrochim. Acta A Mol. Biomol. Spectrosc., 2012, 96, 340, doi:10.1016/j.saa.2012.05.050
- [37] Lakshmi A., and Balachandran V., J. Mol. Struct., 2013, 1033, 40-50, doi:10.1016/j.molstruc.2012.08.002
- [38] Ramalingama S., Karabacak M., Periandy S., Puviarasan N., and Tanuja D., Spectrochim. Acta A Mol. Biomol. Spectrosc., 2012, 96, 207, doi:10.1016/j.saa.2012.03.090
- [39] Fleming I., Frontier Orbitals and Organic Chemical Reactions, John Wiley & Sons, New York ,pp. 5,(1976).
- [40] Murray J.S., Sen K., Molecular Electrostatic Potentials, Concepts and Applications, Elsevier, Amsterdam, (1996).
- [41] Alkorta I., Perez J., Molecular polarization potential maps of the nucleic acid bases., Int. J. Quant. Chem., 1996, 57, 123.
- [42] Scrocco E., Tomasi J., Adv. Quantum Chem., 1978, 11. 115–193, doi: 10.1016/s0065-3276(08)60236-1
- [43] Luque F. J., J. Phys. Chem, 1993, 97, 9380, doi : 10.1063/1.467032
- [44] Sponer J., and Hobza P., DNA base amino groups and their role in molecular interactions: Ab initio and preliminary density functional theory calculations., Int. J. Quant. Chem., 1996, 57, 959.
- [45] Mellaoui M., Belaidi S., Bouzidi D., Gherraf N., Quantum Matter., 2014, 3(5), 435-441, doi : 10.1166/qm.2014.1142
- [46] Materska M., Quercetin and its Derivatives: Chemical Structure and Bioactivity, Pol. J. Food Nutr. Sci. 2008, 58(4), 407–413

- [47] Ooi T., Oobatake M., Nemethy G., Scheraga H.A., Proc. Natl. Acad. Sci., 1987, 84, 3086-3090, doi: 10.1073/pnas.84.10.3086
- [48] Akgül, Ö., Tarikoğulları A. H., Köse, F. A., Kirmizibayrak P. B., and Pabuççuoğlu M. V., Synthesis and cytotoxic activity of some 2-(2, 3-dioxo-2, 3-dihydro-1H-indol-1-yl) acetamide derivatives, Turk. J. Chem., 2013, 37(2), 204-212,
- [49] Schultes S., Graaf C., Haaksma E., Iwan J.P, and Kramer O., Drug Discov. Today, Technol., 2010, 7, 157, doi: 10.1016/j.ddtec.2010.11.003
- [50] Kerassa A., Belaidi S., Lanez T., Quantum Matter., 2016, 5, 1, doi:10.1166/qm.2016.1253
- [51] Almi Z., Belaidi S., Segueni L., Rev. Theor. Sci., 2015, 3, 264-272, doi: 10.1166/rits.2015.1038
- [52] Wang, J., Xie, X. Q., Hou, T., & Xu, X. Fast approaches for molecular polarizability calculations, J. Phys. Chem. A, 2007, 111(20), 4443-4448.
- [53] Ouassaf M., Belaidi S., Al Mogren M.M., Chtita S., Khan S.U., Htar T.T., J. King Saud Univ. Sci., 2021, 101352, doi:10.1016/j.jksus.2021.101352
- [54] Andrası M., Buglyo P., Zekany L., and Gaspar A J. Pharm. Biomed. Anal., 2007, 1040, doi: 10.1016/j.jpba.2007.04.024
- [55] Ertl P., Rohde B., and Selzer P., J. Med. Chem., 2000, 43, 3714, doi: 10.1021/jm000942e
- [56] Viswanadhan V.N., Ghose A.K., Revankar G.R., Robins R.K., J. Chem. Inf. Comput. Sci., 1989, 29, 163-172, doi:10.1021/ci00063a006
- [57] Lipinski C.A., Lombardo F., Dominy B.W., and Feeney P., J. Adv. Drug Deliv. Rev., 2012, 4, 17, doi: 10.1016/j.addr.2012.09.019
- [58] Vistoli G., Pedretti A., and Testa B., Drug. Discov. Today, 2008, 13, 285, doi: 10.1016/j.drudis.2007.11.007
- [59] Almi Z., Belaidi S., Melkemi N., Boughdiri S., Belkhiri L., Quantum.Matter. 2016, 5, 124, doi : <https://doi.org/10.1166/qm.2016.1264>
- [60] Lipinski C.A., Lombardo F., Dominy B.W., and P.J., Adv. Drug. Deliv. Rev., 1997, 23, 3, doi: 10.4236/jbise.2010.34051